Accounting for vertical and horizontal turbulent mixing in a three-dimensional planetary boundary layer parameterization

Pedro Jimenez Muñoz[1] and Branko Kosović[1]
Timothy Juliano[1], Masih Eghdami[2], Alberto Martilli[3], and Ana Barros[2]

Meteorology and Climate – Modeling for Air Quality Conference 2019
UC Davis, September 11-13, 2019

1 – NCAR,
2 – Duke University
3 – CIEMAT, Spain

Motivation

- High spatial resolution is required to achieve more accurate representation of surface heterogeneities such as the complexity of the complex terrain, however…
- Currently NWP models use 1D planetary boundary layer (PBL) parameterizations that assume horizontal homogeneity
- Horizontal homogeneity is not valid in complex terrain in ”gray zone” (“Terra Incognita”) range ~100 m to 1- 2 km
- There were attempts to address this issue by developing “scale aware” PBL parameterizations
- The goal is to develop and implement a three-dimensional planetary boundary layer scheme based on first principles

What is an effective approach to simulating mesoscale-microscale interactions?

Fiori et al. 2010, 2011
Beare 2013
Boutle et al. 2014
Shin and Hong 2013, 2015
Shin and Dudhia 2016
Zhang et al. 2018
etc.

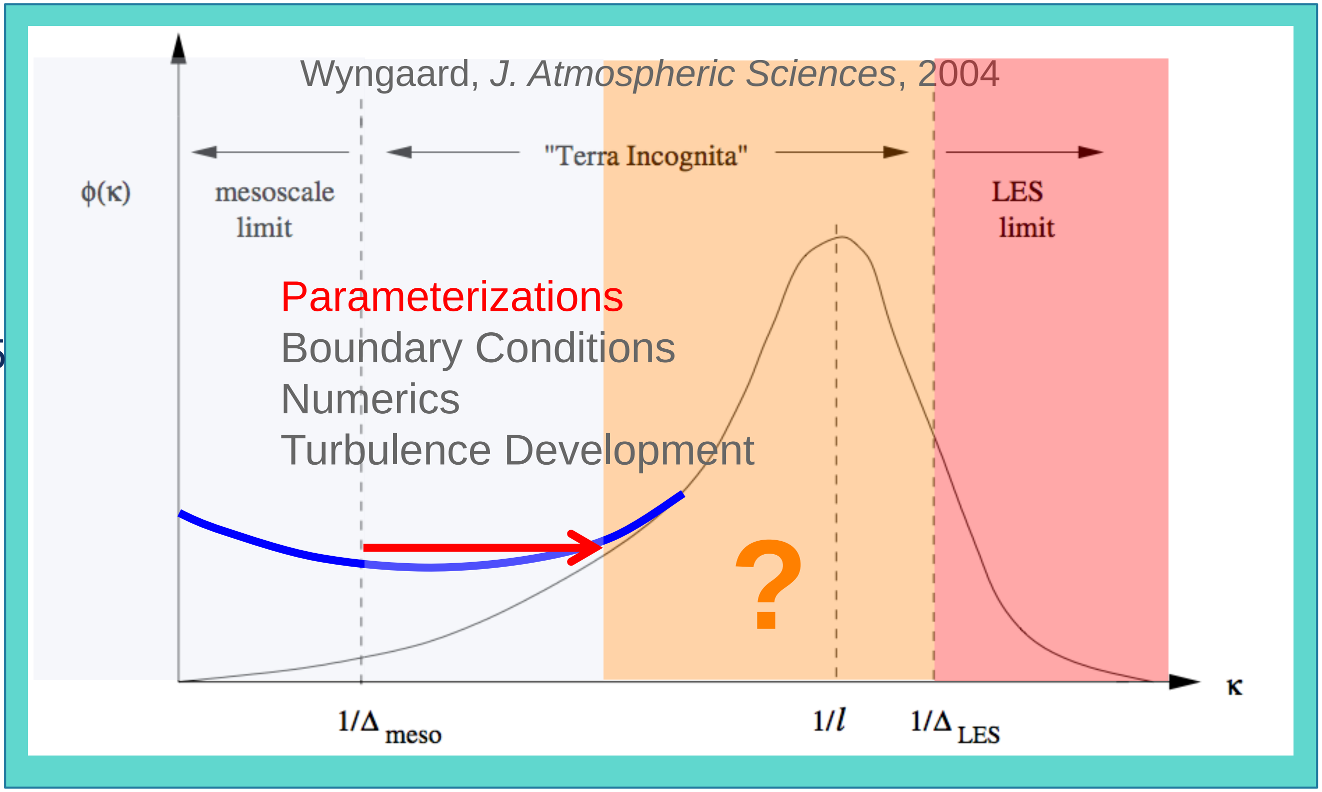

Hommert and Masson 2014 indicate that horizontal motions must be represented at
dx = 0.5 times the PBL height in free convection and
dx = 3 times the PBL height in forced convection
under a cloud free boundary layer

NCAR | UCAR

Why a 3D PBL scheme?

Conservation equation for the horizontal wind components:

$$\frac{\partial U}{\partial t} + U_j \frac{\partial U}{\partial x_j} = -\frac{1}{\rho}\frac{\partial P}{\partial x} - fV - \frac{\partial \langle uw \rangle}{\partial z}$$

$$\frac{\partial V}{\partial t} + U_j \frac{\partial V}{\partial x_j} = -\frac{1}{\rho}\frac{\partial P}{\partial y} + fU - \frac{\partial \langle vw \rangle}{\partial z}$$

- 1D PBL closure is based on the assumption of homogeneity over a grid cell
- Vertical turbulent fluxes are parameterized by the PBL scheme (e.g., MYNN, YSU, etc.)
- Horizontal diffusion is parameterized using 2D Smagorinsky type model (Smagorinsky 1963)
- 2D Smagorinsky model is introduced for numerical stability

3D PBL mixing better represents turbulent fluxes

Conservation equation for the velocity components:

$$\frac{\partial U_i}{\partial t} + U_j \frac{\partial U_i}{\partial x_j} = -\frac{1}{\rho}\frac{\partial P}{\partial x_i} + 2\epsilon_{ijk}\Omega_j U_k - \frac{\partial \langle u_i u_j \rangle}{\partial x_j}$$

- 3D PBL scheme includes (diagnostic) parameterization of all six turbulent stress components and computation of stress divergence (Mellor and Yamada 1974,1982; Yamada and Mellor 1975)
- Consistent closure assumption for all stress components

The 3D PBL scheme for turbulent stresses and fluxes based on algebraic system

Solving system of linear algebraic equations requires TKE and a “master” length scale (Mellor and Yamada 1974, 1982; Yamada and Mellor 1975).

$$
\begin{bmatrix}
\frac{q}{2\ell_1}+2\frac{\partial U}{\partial x} & -\frac{\partial V}{\partial y} & -\frac{\partial W}{\partial z} & 2\frac{\partial U}{\partial y}-\frac{\partial V}{\partial x} & 2\frac{\partial U}{\partial z}-\frac{\partial W}{\partial x} & -\frac{\partial V}{\partial z}-\frac{\partial W}{\partial y} & 0 & 0 & \beta g & 0 \\
-\frac{\partial U}{\partial x} & \frac{q}{2\ell_1}+2\frac{\partial V}{\partial y} & -\frac{\partial W}{\partial z} & 2\frac{\partial V}{\partial x}-\frac{\partial U}{\partial y} & -\frac{\partial U}{\partial z}-\frac{\partial W}{\partial x} & 2\frac{\partial V}{\partial z}-\frac{\partial W}{\partial y} & 0 & 0 & \beta g & 0 \\
-\frac{\partial U}{\partial x} & -\frac{\partial V}{\partial y} & \frac{q}{2\ell_1}+2\frac{\partial W}{\partial z} & -\frac{\partial U}{\partial y}-\frac{\partial V}{\partial x} & 2\frac{\partial W}{\partial x}-\frac{\partial U}{\partial z} & 2\frac{\partial W}{\partial x}-\frac{\partial V}{\partial z} & 0 & 0 & -2\beta g & 0 \\
\frac{\partial V}{\partial x} & \frac{\partial U}{\partial y} & 0 & \frac{q}{3\ell_1}+\frac{\partial U}{\partial x}+\frac{\partial V}{\partial y} & \frac{\partial V}{\partial z} & \frac{\partial U}{\partial z} & 0 & 0 & 0 & 0 \\
\frac{\partial W}{\partial x} & 0 & \frac{\partial U}{\partial z} & \frac{\partial W}{\partial y} & \frac{q}{3\ell_1}+\frac{\partial U}{\partial x}+\frac{\partial W}{\partial z} & \frac{\partial U}{\partial y} & -\beta g & 0 & 0 & 0 \\
0 & \frac{\partial W}{\partial y} & \frac{\partial V}{\partial z} & \frac{\partial W}{\partial x} & \frac{\partial V}{\partial x} & \frac{q}{3\ell_1}+\frac{\partial V}{\partial y}+\frac{\partial W}{\partial z} & 0 & -\beta g & 0 & 0 \\
\frac{\partial \Theta}{\partial x} & 0 & 0 & \frac{\partial \Theta}{\partial y} & \frac{\partial \Theta}{\partial z} & 0 & \frac{q}{3\ell_2}+\frac{\partial U}{\partial x} & \frac{\partial U}{\partial y} & \frac{\partial U}{\partial z} & 0 \\
0 & \frac{\partial \Theta}{\partial y} & 0 & \frac{\partial \Theta}{\partial x} & 0 & \frac{\partial \Theta}{\partial z} & \frac{\partial V}{\partial x} & \frac{q}{3\ell_2}+\frac{\partial V}{\partial y} & \frac{\partial V}{\partial z} & 0 \\
0 & 0 & \frac{\partial \Theta}{\partial z} & 0 & \frac{\partial \Theta}{\partial x} & \frac{\partial \Theta}{\partial y} & \frac{\partial W}{\partial x} & \frac{\partial W}{\partial y} & \frac{q}{3\ell_2}+\frac{\partial W}{\partial z} & -\beta g \\
0 & 0 & 0 & 0 & 0 & 0 & \frac{\partial \Theta}{\partial x} & \frac{\partial \Theta}{\partial y} & \frac{\partial \Theta}{\partial z} & \frac{q}{\Lambda_2}
\end{bmatrix}
\begin{bmatrix}
\overline{u^2} \\ \overline{v^2} \\ \overline{w^2} \\ \overline{uv} \\ \overline{uw} \\ \overline{vw} \\ \overline{u\theta} \\ \overline{v\theta} \\ \overline{w\theta} \\ \overline{\theta^2}
\end{bmatrix}
=
\begin{bmatrix}
\frac{q^3}{6\ell_1}+3C_1q^2\frac{\partial U}{\partial x} \\
\frac{q^3}{6\ell_1}+3C_1q^2\frac{\partial V}{\partial y} \\
\frac{q^3}{6\ell_1}+3C_1q^2\frac{\partial W}{\partial z} \\
C_1q^2\left(\frac{\partial V}{\partial x}+\frac{\partial U}{\partial y}\right) \\
C_1q^2\left(\frac{\partial W}{\partial x}+\frac{\partial U}{\partial z}\right) \\
C_1q^2\left(\frac{\partial W}{\partial y}+\frac{\partial V}{\partial z}\right) \\
0 \\ 0 \\ 0 \\ 0
\end{bmatrix}
$$

At each grid cell this system of algebraic equations is solved using either Gaussian elimination or sequential over-relaxation method.

We compare simulations with 1D and 3D PBLs for an idealized case of heterogeneous surface heat flux

- 8km x 8km domain,
- Gird-cell size: dx=200 m
- Light winds from south
  - $u=0$ m s^{-1}, $v=2$ m s^{-1}
- Surface sensible heat flux)
  - x <= 4km, SHF = 160 W m^{-2}
  - x > 4 km, SHF = 320 W m^{-2}

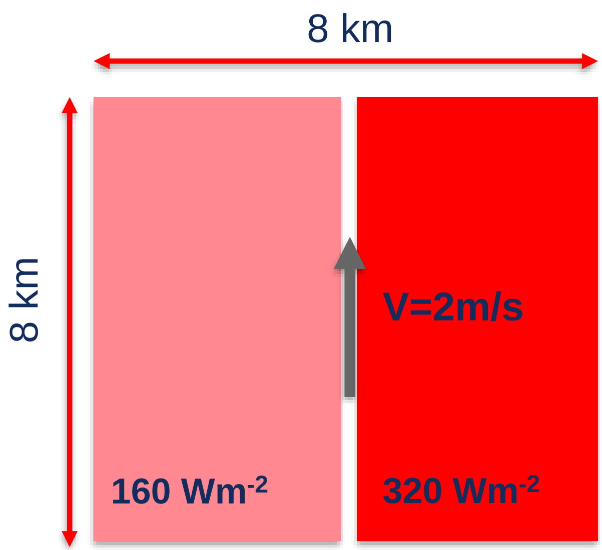

We compare 1D and 3D PBLs for simple case of contrasting surface heat flux

1D PBL generates artificial spurious structures in **streamwise velocity**, while 3D PBL convection shows evidence of appropriate narrow updraft

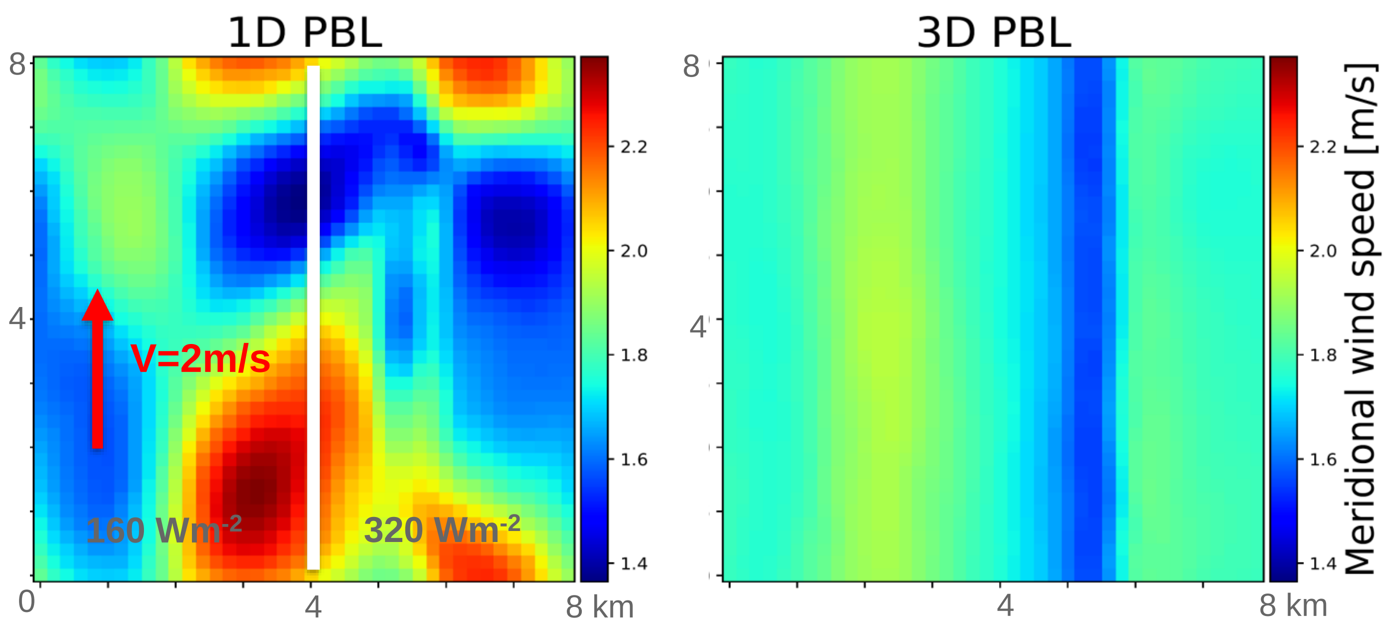

We compare 1D and 3D PBLs for simple case of contrasting surface heat flux

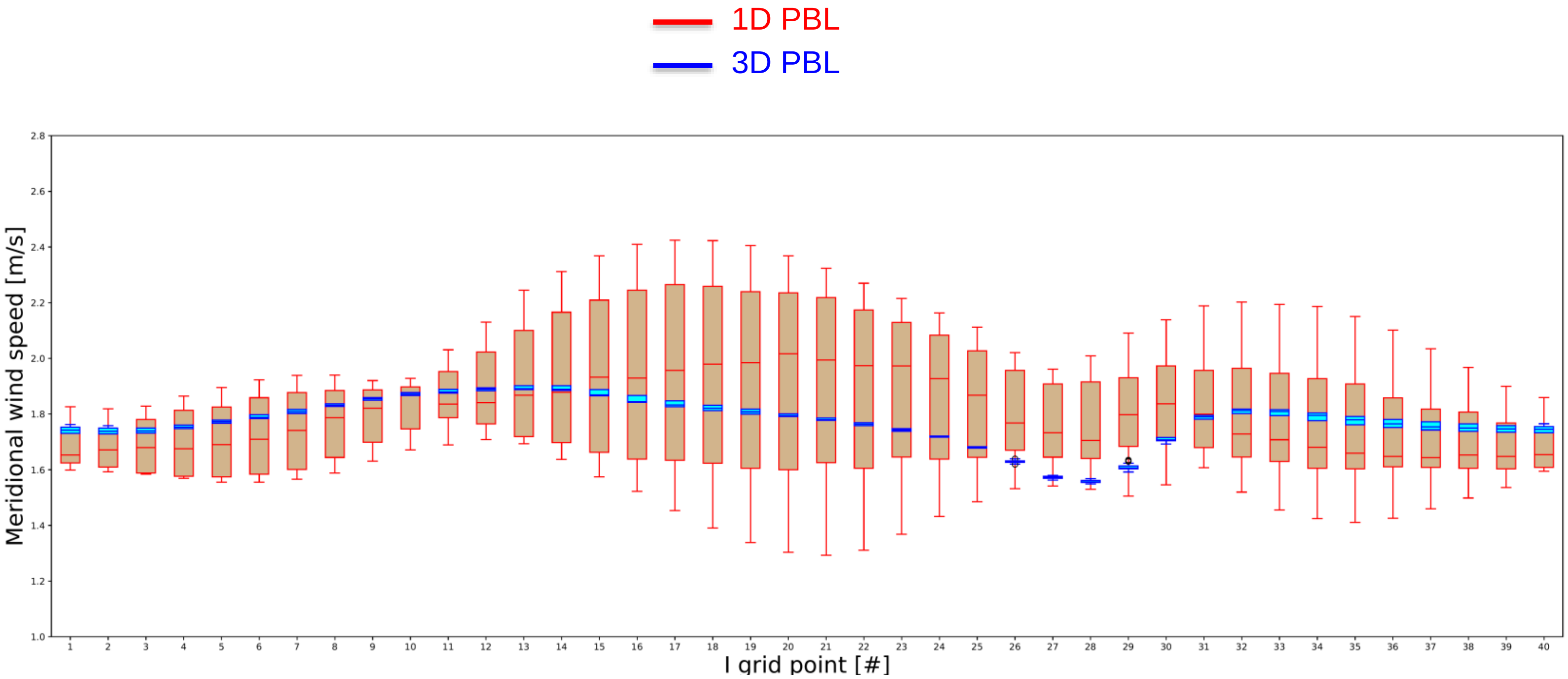

We compare 1D and 3D PBLs for simple case of contrasting surface heat flux

1D PBL generates artificial spurious structures in **vertical velocity**, while 3D PBL convection shows evidence of appropriate narrow updraft

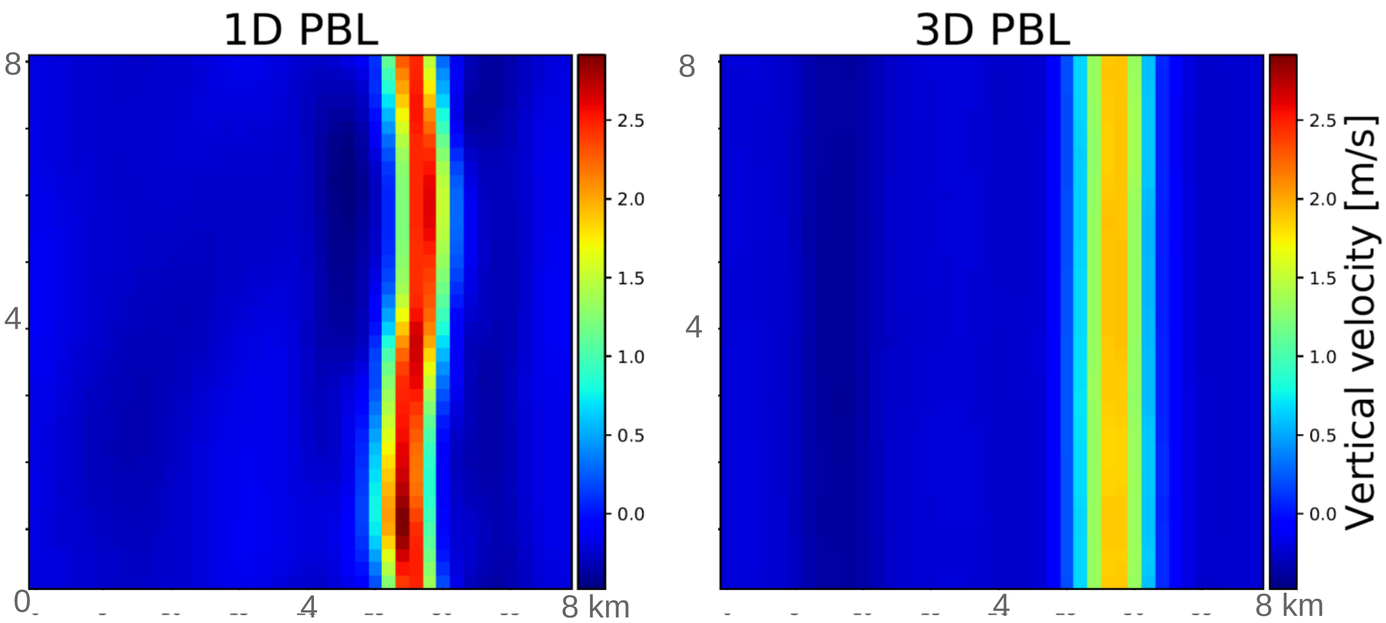

We compare 1D and 3D PBLs for simple case of contrasting surface heat flux

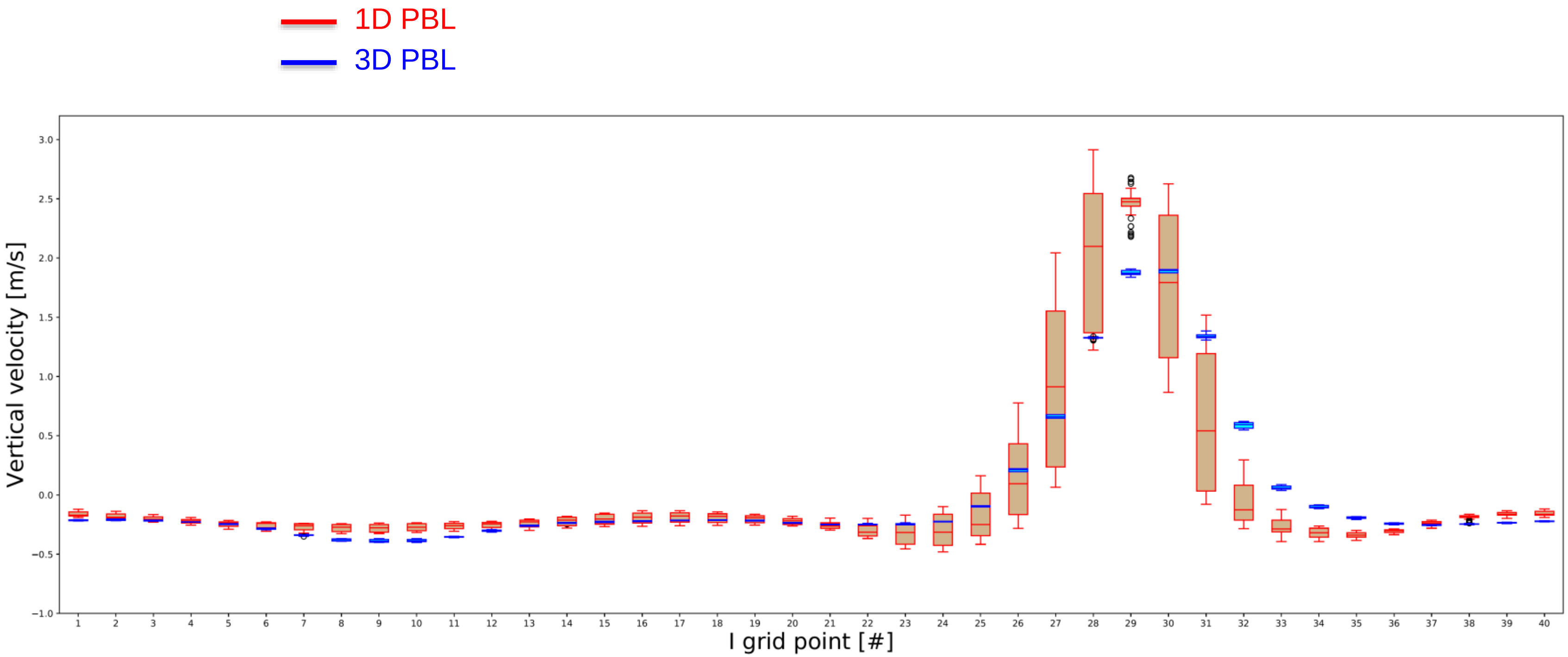

We compare 1D and 3D PBLs for simple case of contrasting surface heat flux

The ensemble mean of 20 LES of heterogeneous convective ABL converges to a weaker updraft similar to the 3D PBL simulation result.

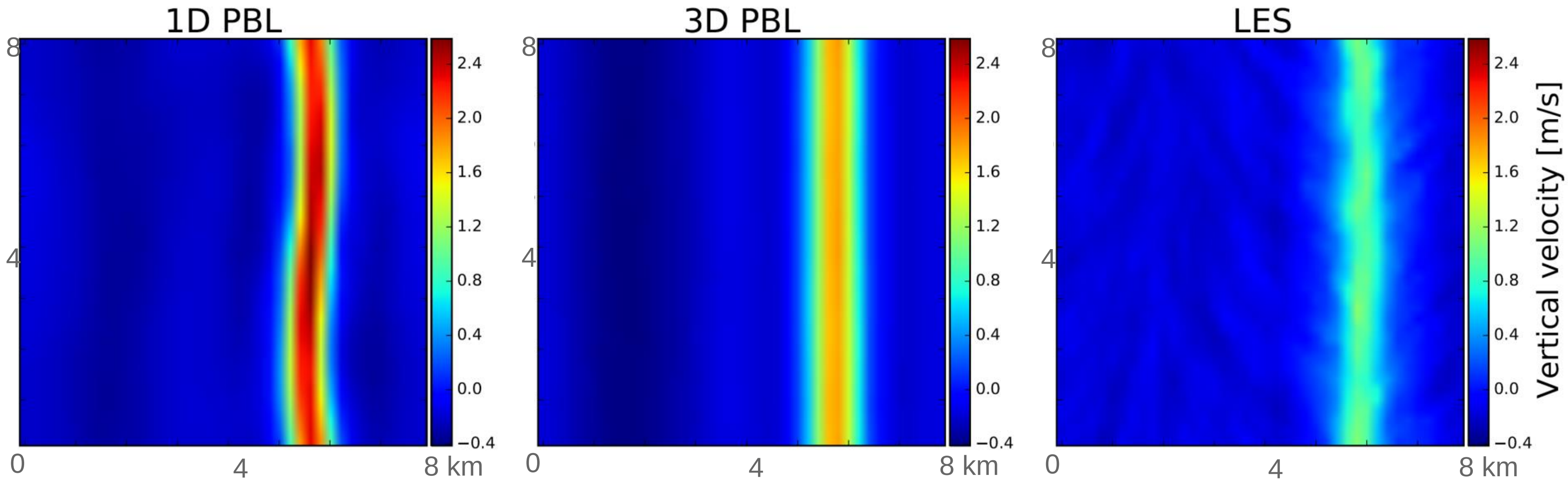

We are Testing the 3D PBL Parameterization and LES Based on WFIP2 Observations

The 3D PBL simulation domains are smaller to enable faster simulations and avoid steep slopes that present a problem for terrain following coordinates.

Columbian River Gorge – Oregon – LES Domains

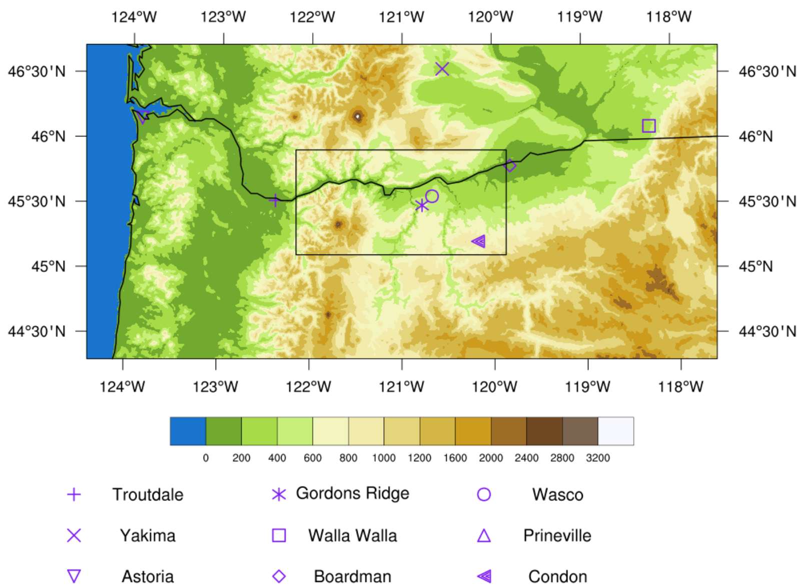

D01 – 90 m, D02 – 30 m. grid-cell size

3D PBL Domains

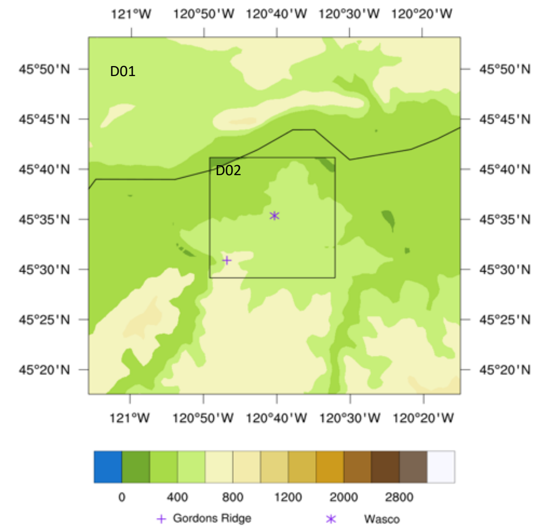

D01 – 750 m, D02 – 250 m grid-cell size

The effect of 3D PBL with or without horizontal diffusion on temperature and wind speed is subtle

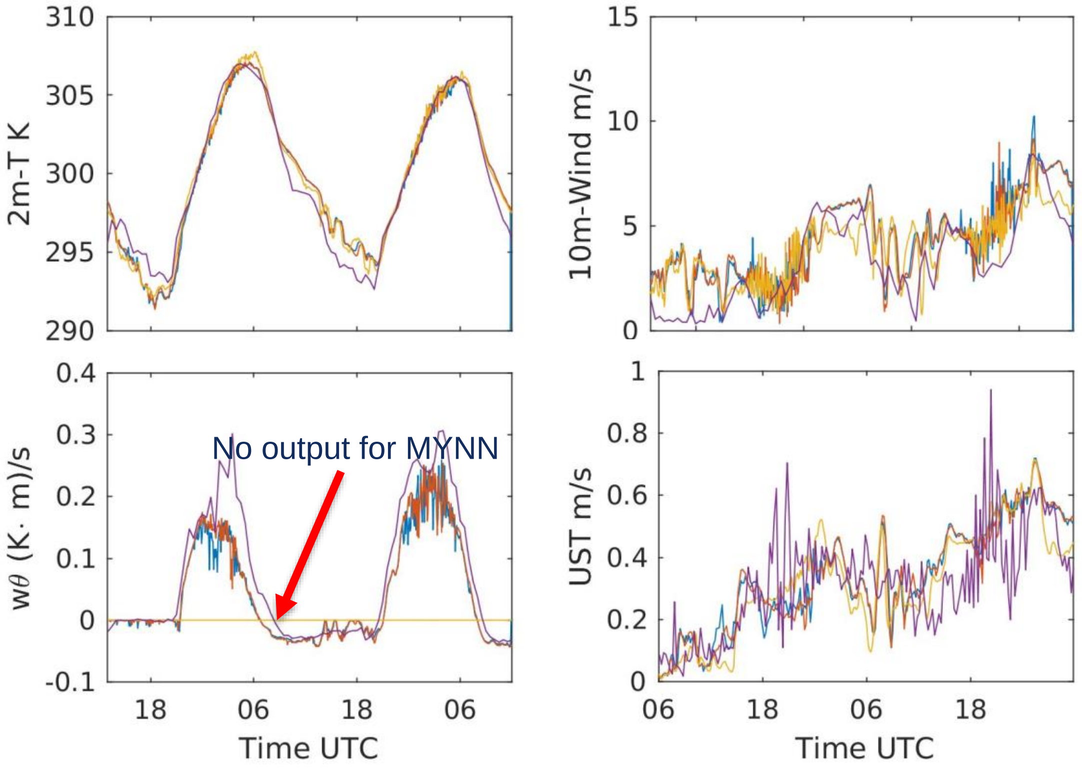

Blue – 3D PBL w. 2D Smagorinsky
Red – 3D PBL
Orange – 1D MYNN
Black - Observations

3D PBL captures vertical shear but horizontal shear is underpredicted

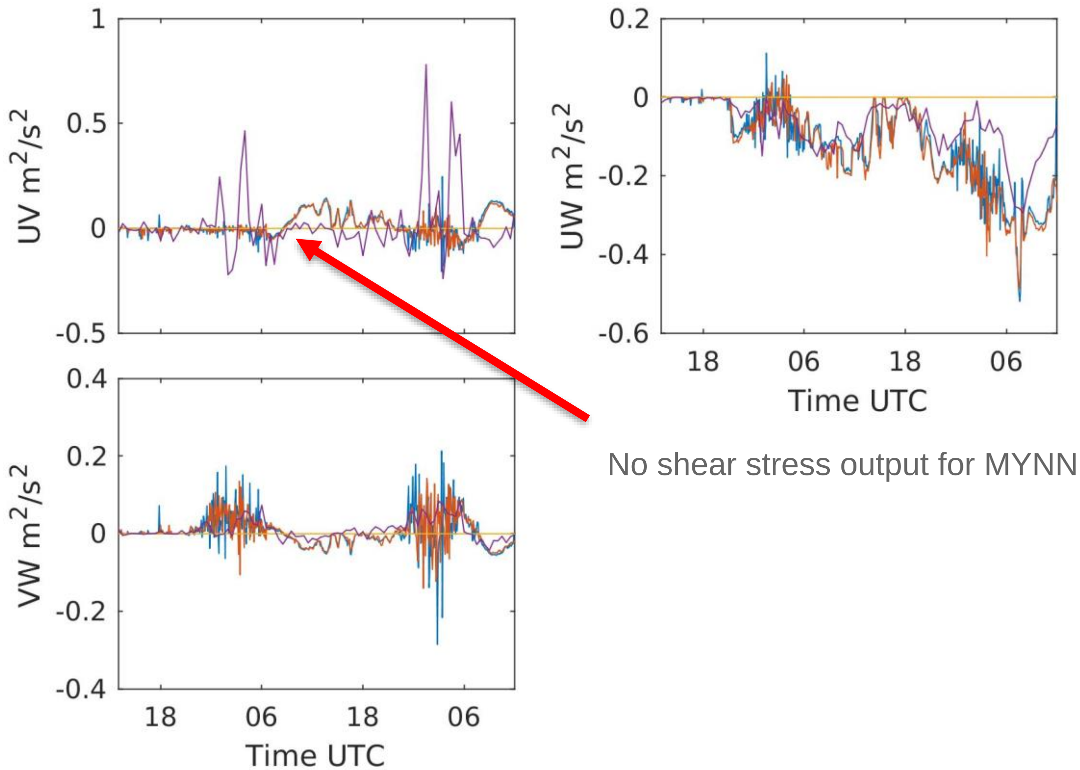

No shear stress output for MYNN

Blue – 3D PBL w. 2D Smagorinsky
Red – 3D PBL
Orange – 1D MYNN
Black - Observations

1D PBL lacks variances while 3D PBL overpredicts vertical and underpredicts horizontal variances

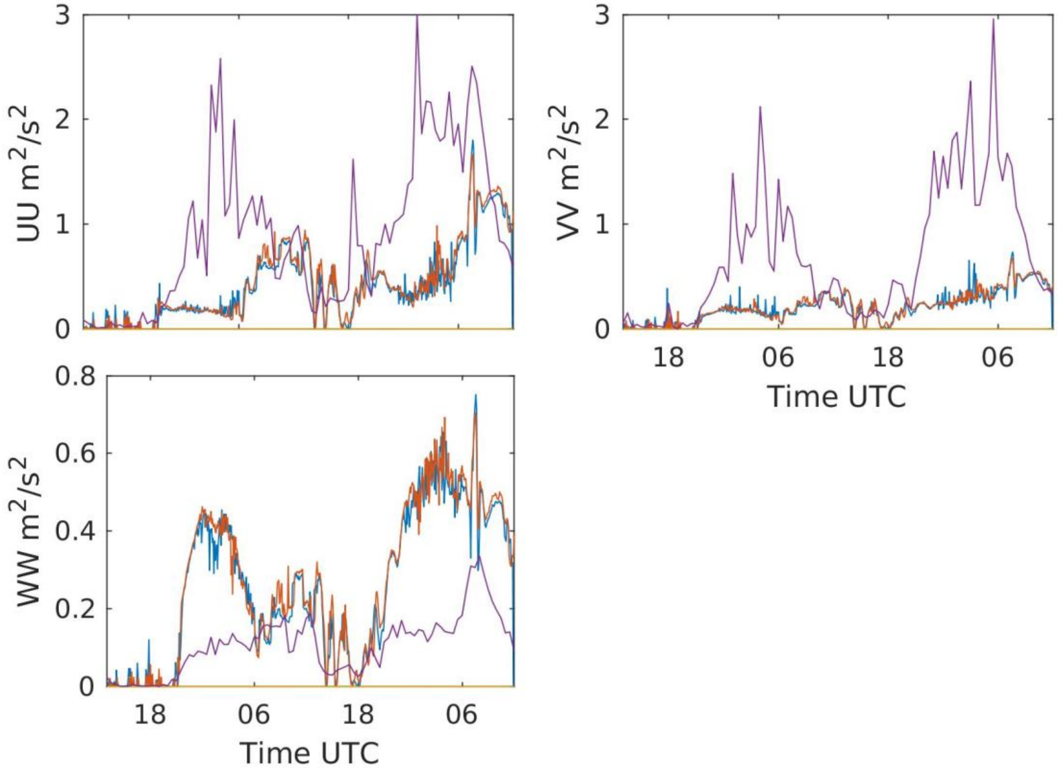

Blue – 3D PBL w. 2D Smagorinsky
Red – 3D PBL
Orange – 1D MYNN
Black - Observations

LES domains over the WFIP2 field study area

WRF – Domain 1 – grid-cell size 90 m; Domain 2 – grid-cell size 30 m

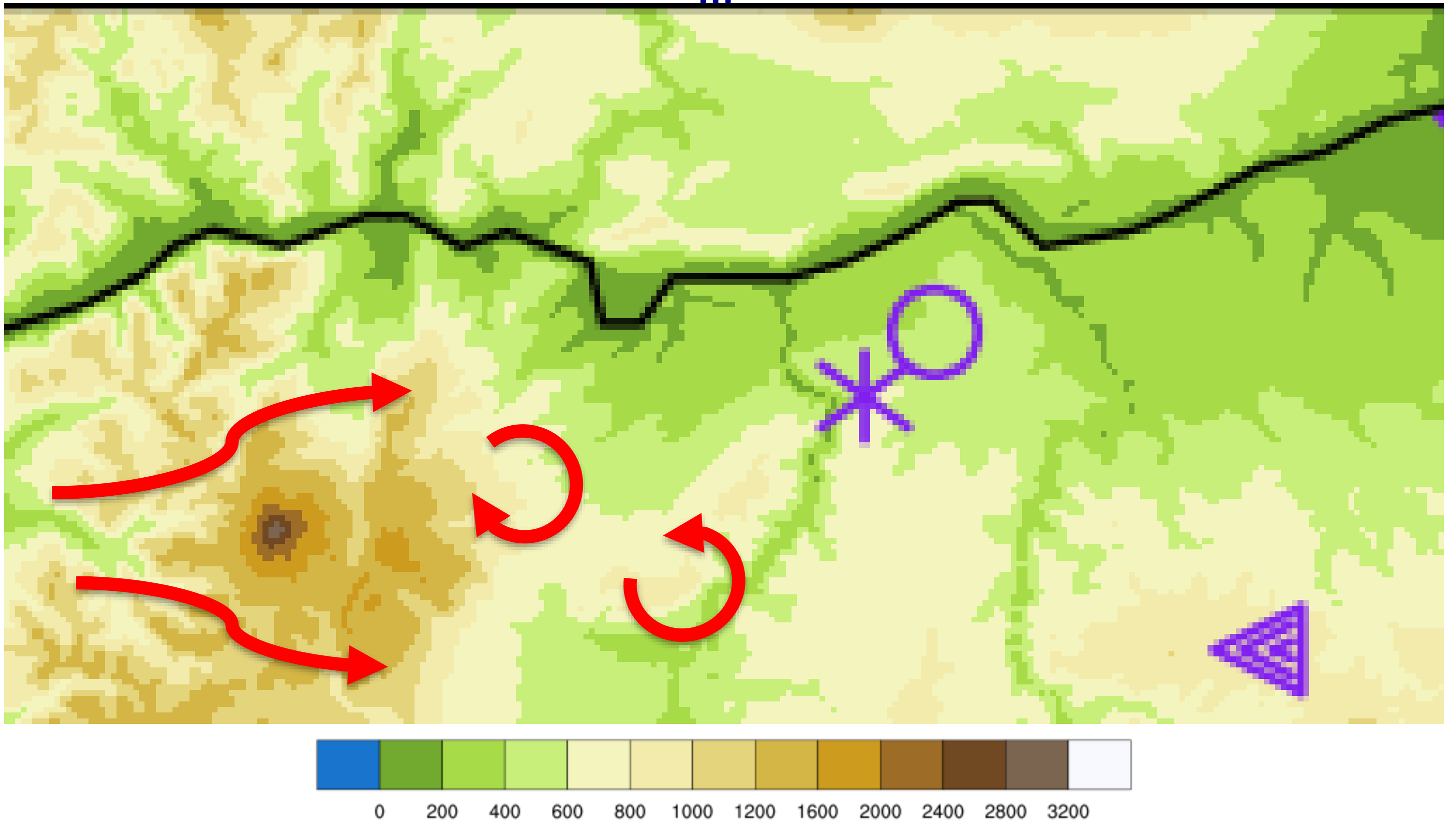

NCAR | UCAR

High-resolution, large-eddy simulations are used to improve numerical weather prediction models

Horizontal velocity

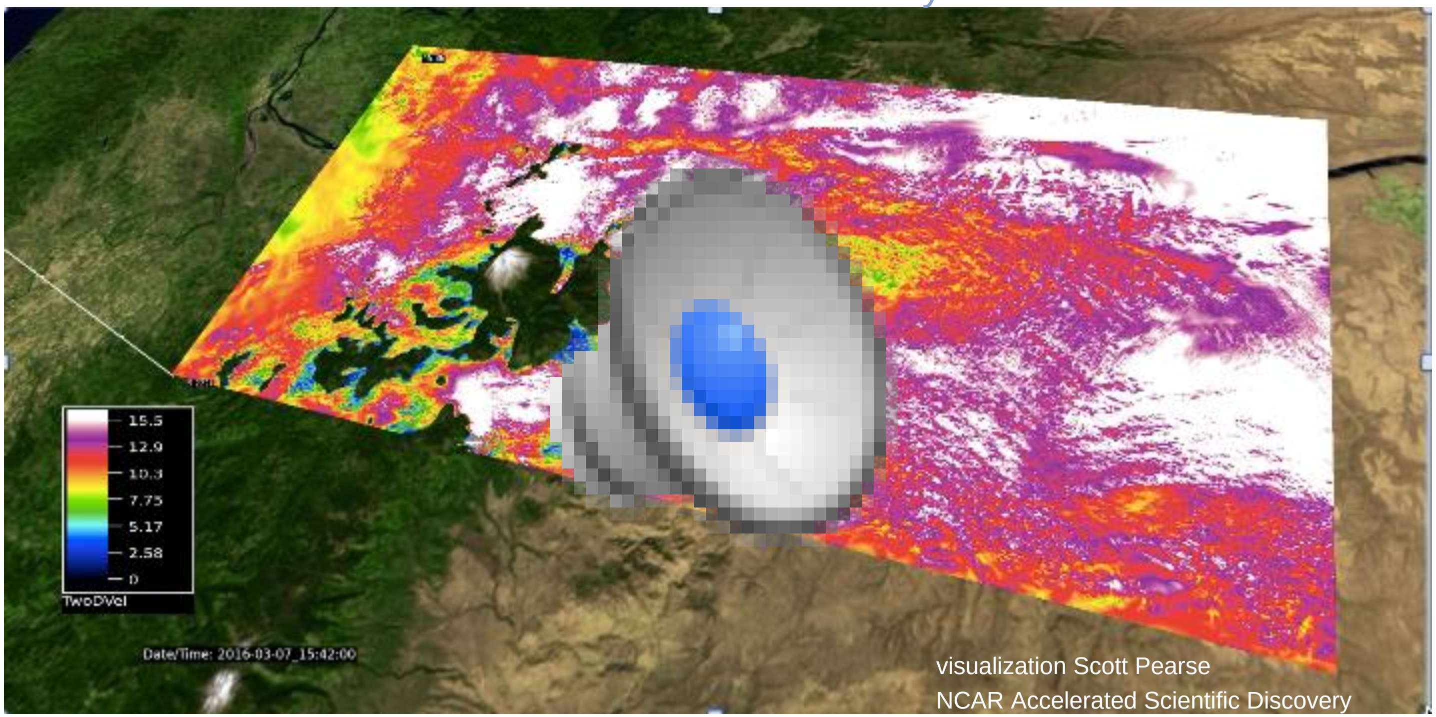

Topographic wake and gap flow observed on March 07 – 08, 2016

High-resolution, large-eddy simulations are used to improve numerical weather prediction models

Vertical velocity

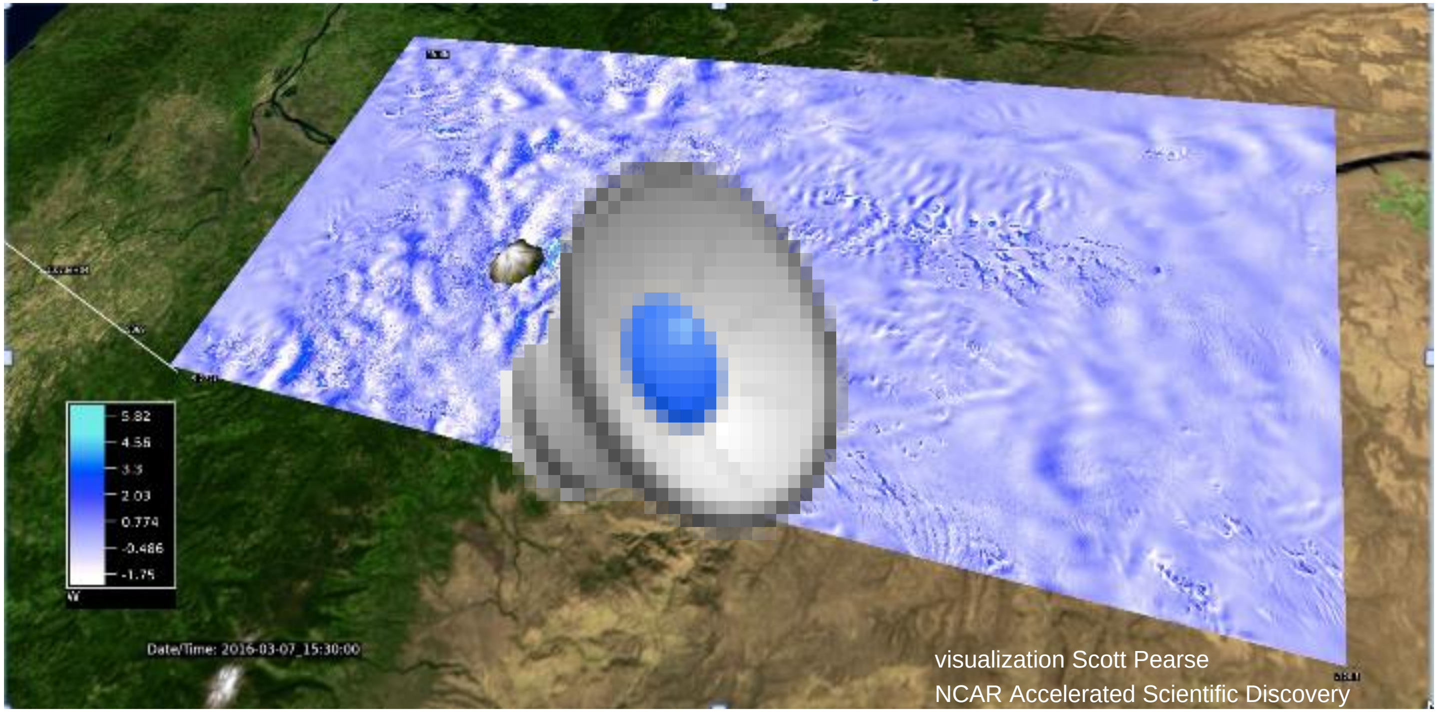

Topographic wake and mountain waves observed on March 07 – 08, 2016

AON5 Sodar

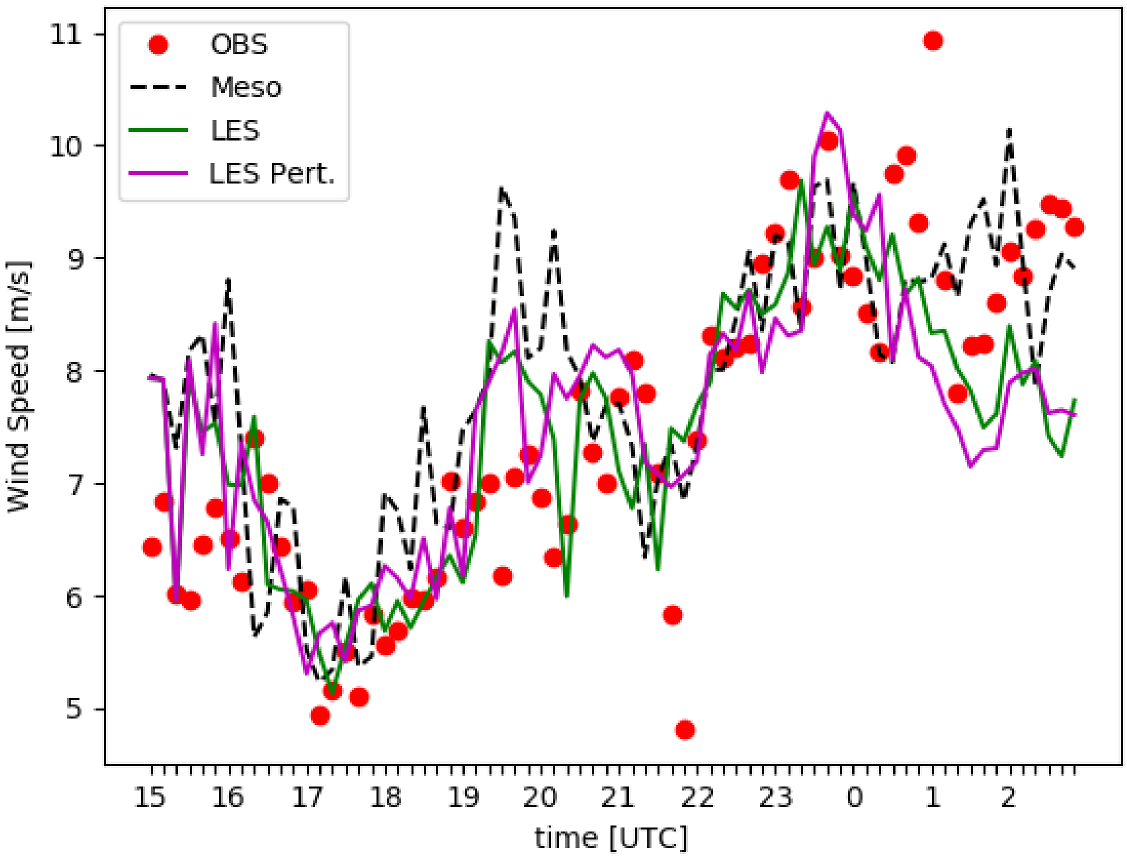

OBS
Meso
LES
LES Pert.
Wind Speed [m/s]
11
10
9
8
7
6
5
15
16
17
18
19
20
21
22
23
0
1
2
time [UTC]

Mean Absolute Error [m s^{-1}]				
	Mesoscale 1D PBL	LES	LES w. cell perturbation	LES w. cell perturbation and hybrid advection
AON2	2.56	**2.26**	2.31	2.36
AON4	1.63	**1.14**	1.18	1.15
AON5	0.89	**0.75**	0.84	0.79
AON6	**2.45**	2.47	2.60	**2.45**
AON7	**2.14**	2.20	2.16	2.24
AON8	2.70	2.73	**2.63**	**2.63**

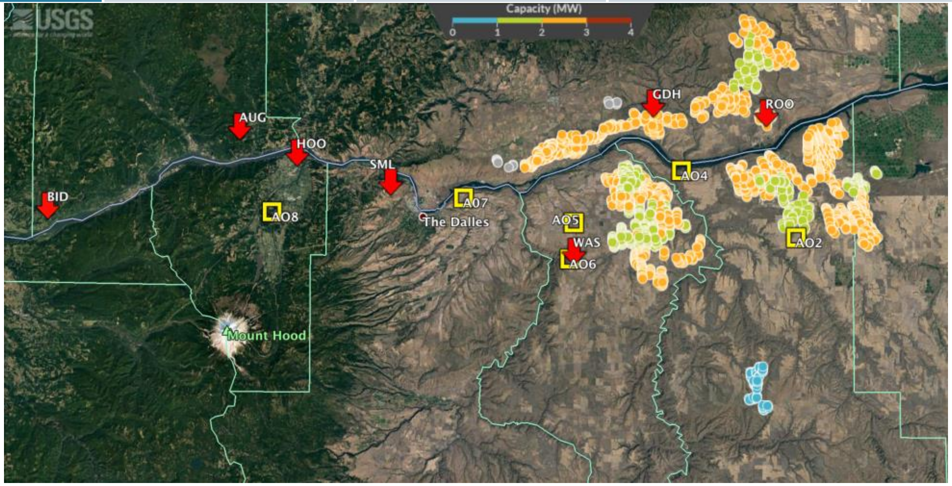

Summary

- 3D PBL was implemented in WRF, however development and validation is work in progress
- 3D PBL parameterization eliminates undesirable effects of 1D PBL schemes in high resolution mesoscale simulations of convective boundary layers
- 3D PBL parameterization produces results that are similar to an ensemble of LES
- Early results with 3D PBL suggest that it improves prediction

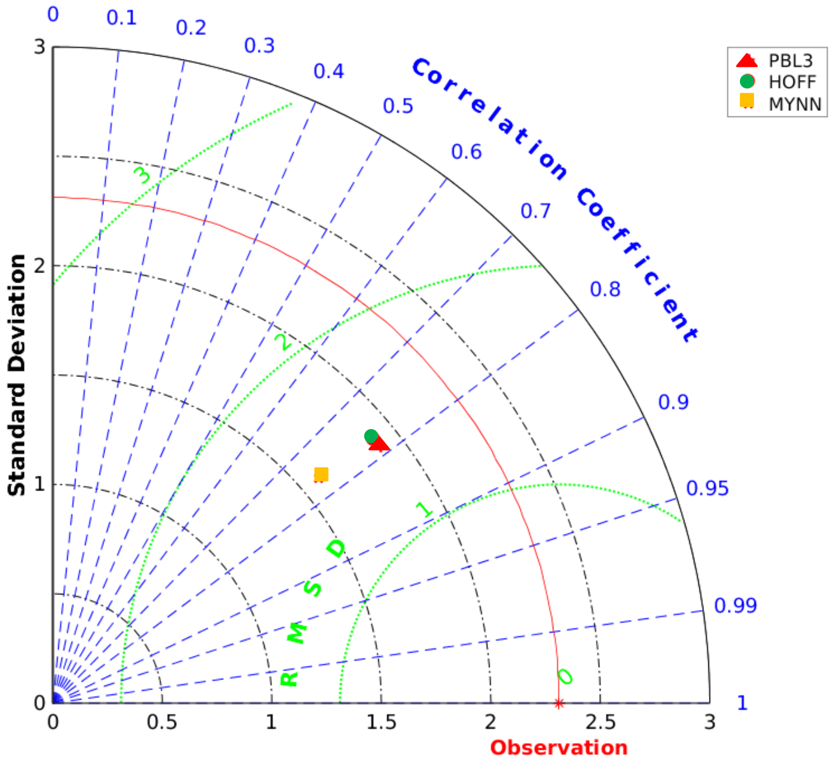

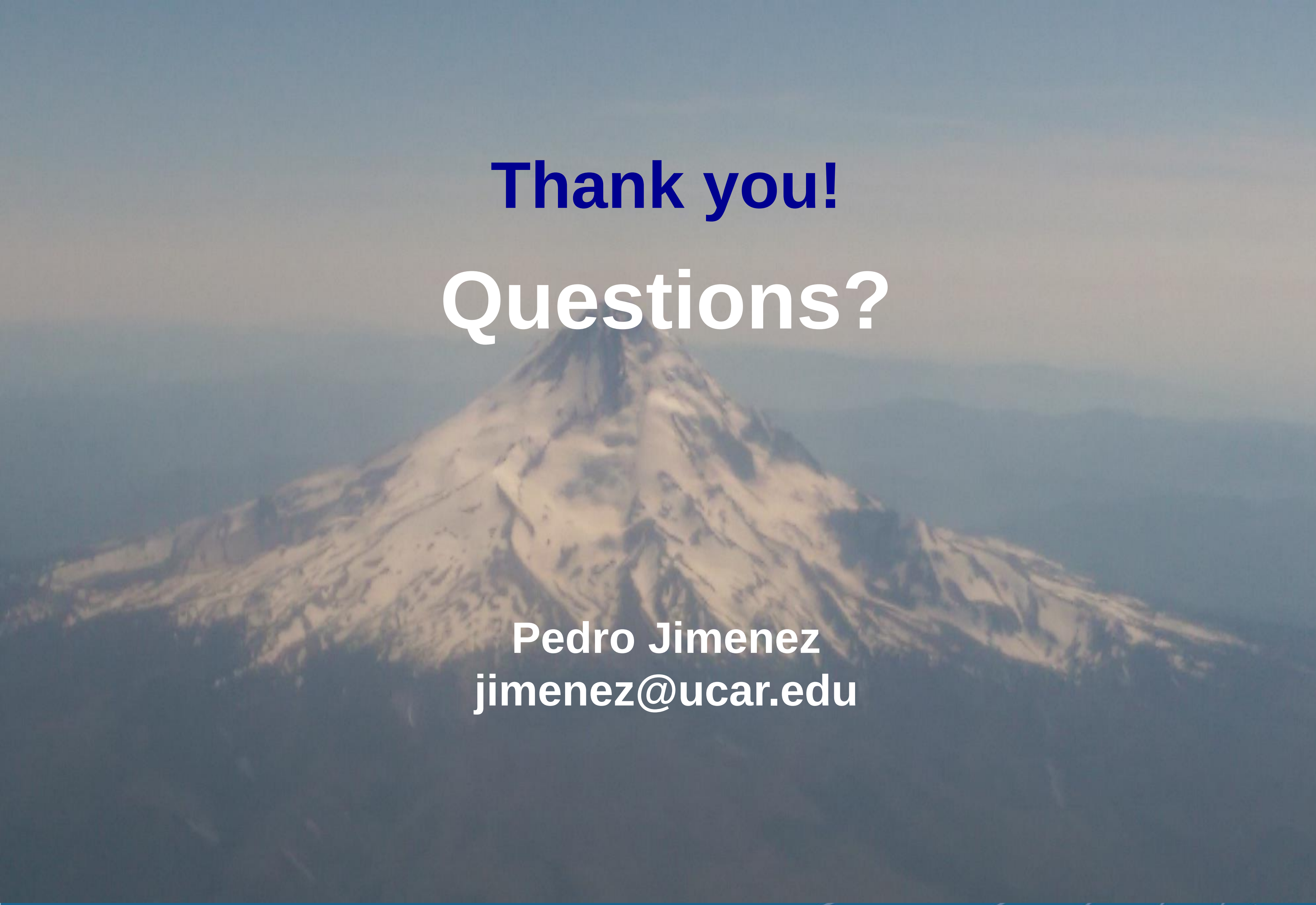

Thank you!

Questions?

Pedro Jimenez
jimenez@ucar.edu